Recent LHCD experiments in EAST

B J Ding, EAST Team and Collaboration Team

Institute of Plasma Physics, Chinese Academy of Sciences, Hefei, 230031, China

Abstract: LHCD system of 2.45 GHz in EAST has been updated to 4MW in last campaign. Aimed at high confinement (H-mode) plasma in EAST, the LHW-plasma coupling and current drive experiments were continued. Experiments of local gas puffing near LHW antenna shows that gas puffing from electron side is better to improve LHW-plasma coupling than that from ion side. LHCD experiments at high density are also performed, demonstrating that the decrease of current efficiency at high density may be related to the parametric decay instability (PDI) effect. Lithiation and local gas puffing near LHW antenna are utilized so as to sustain H-mode plasma. H-mode plasma is obtained by LHCD with a wide range of parameters: Ip=0.4~0.8MA, B_t=1.35~1.81T, n_e=1.5~2.5x10^{19} m^{-3}, P_{LHW}>=0.5MW. LHW power deposition and driven current profile with C3PO/LUKE are calculated with the experimental parameters, showing that central and large driven current seems not a necessary condition for the H-mode plasma. H-mode is reproduced with CRONOS. Long pulse plasmas, >400s L mode fully driven by LHCD and >30s H-mode with LHCD and ICRF, have been achieved and demonstrated in EAST.

Key words: coupling, LHCD, PDI, H-mode

1. Introduction

Lower hybrid current drive (LHCD) [1-3] plays a key role in controlling current profile in tokamak experiments aimed at achieving important goals relevant to fusion plasma. Good lower hybrid wave (LHW)-plasma coupling is the first necessary condition for LHCD experiment and high current drive (CD) efficiency is important for driving plasma current and controlling current profile, especially for sustaining long pulse high confinement (H-mode). Aimed at H-mode plasma in EAST, LHW-plasma coupling and current drive experiments were continued, especially, local gas puffing from electron (GIM_e) and ion side (GIM_i) of LHW antenna and high density experiments with LHCD.

Reactor relevant steady state regimes have faced lower hybrid (LH) with the challenge of effectively penetrating the main plasma without excessive power dissipation in the relatively high density plasma edge. The efficiency of LHCD is predicted to scale with the inverse of the electron density [4]. However, LHCD experiments on many tokamaks [5-8] have observed a decrease in non-thermal tails and a drop in bremsstrahlung emission much steeper than $1/n_e$ at high density, which is stronger than expected based on current models. Some possible mechanisms, individually or simultaneously, have been identified to preclude the penetration of lower hybrid (LH) waves,

dissipating the power in the plasma periphery and degrade LH efficiency: Collisional Absorption (CA) [9], Parametric Decay Instabilities (PDI) [10], Scattering from Density Fluctuations (SDF) [11], and so on.

H-mode has been obtained by means of heating and current drive, including neutral beam injection (NBI), ion cyclotron resonance heating (ICRH), electron cyclotron resonance heating (ECRH) and LHCD [12-15]. Among of them, the mechanism of H-mode generated by LHCD is not clear yet and the related study is not enough compared to others.

Since high density is an inevitable issue in further LHCD, in order to pursue the high performance in EAST, it is necessary to further investigate LHW-plasma coupling, LHCD experiments at high density, and H-mode experiments with LHCD, so as to further understand the physical mechanism.

2. Experimental set-up

EAST is a first full superconducting tokamak with an advanced configuration in the world [16-20]. The superconducting coils can create and maintain a toroidal magnetic field, B_t, of up to 3.5 T in steady state [20]. In EAST, a LHW is launched into the tokamak plasma by a multi-junction grill [21] type of antenna with 5 modules arranged by 5 rows in the poloidal direction.

In order to improve LHW-plasma coupling, two gas pipes covering the total grill in the poloidal direction are installed near the LHW antenna in EAST. One is in the electron side (GIM_e), and the other is in the ion side (GIM_i). The toroidal angle between antenna and pipe is about 33 degree. The layout of top view is shown in Fig .1, in which the positions in radial direction are also shown. The major radius of the pipe location is about 2400mm.

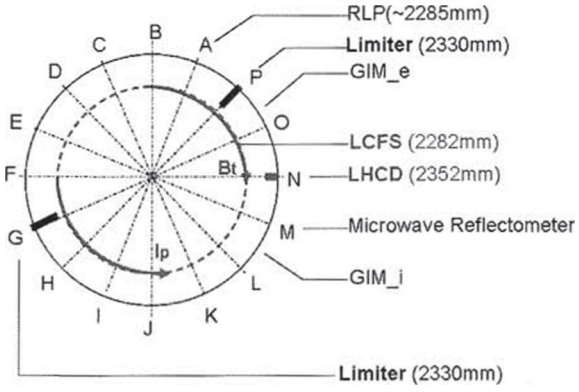

Fig.1 Top view of local gas puffing

3. LHW-plasma coupling experiments

A typical waveform of multi-L-H transitions without local gas puffing is shown in Fig.2. The H-mode phase is characterized by a low D_a with ELM free accompanying high radiation (Prad). It is seen that plasma-wave coupling deteriorates as the transition of L-H occurs, due to the steep gradient density profile in H-mode. The density is then recovered slowly until the H-L transition occurs. This can be seen from the measured density profile in SOL shown in Fig. 3 during L and H mode plasma in another similar discharge. The plasma radiation has a correspondingly periodic characteristic behavior during L-H and H-L transition. Such changes of radiated power and coupled LHW power may lead to the multiple L-H-L transitions, suggesting that the net power for H-mode plasma is marginal. Therefore, it is necessary to reduce

impurity radiation and improve LHW-plasma coupling to sustain H-mode plasma, eg., by means of lithium coating and local gas puffing.

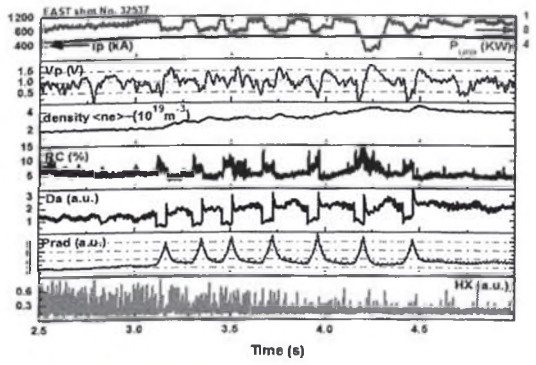

Fig. 2 Typical L-H-L waveform

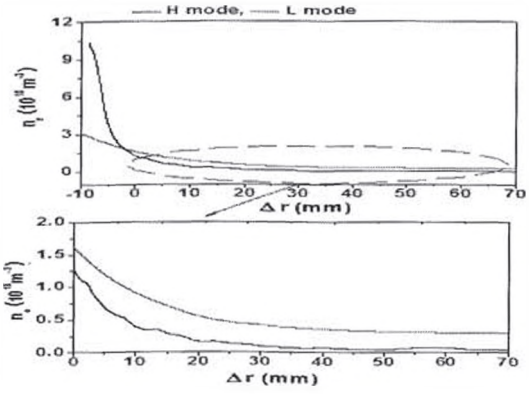

Fig.3 Density profile in SOL

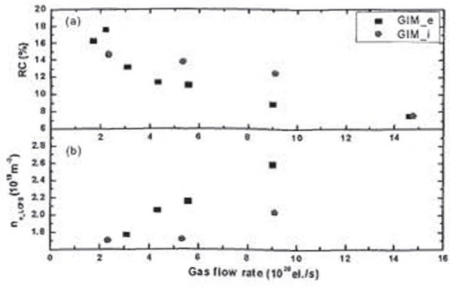

Fig.4 RC and ne_LCFS vs gas flow rate

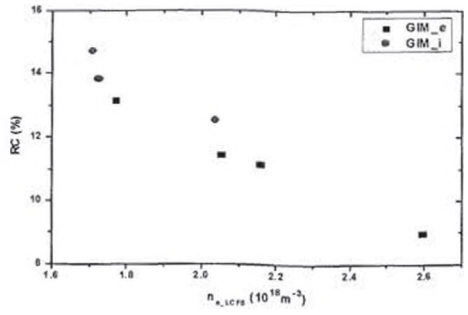

Fig.5 RC vs ne_LCFS first performed in EAST.

In order to investigate the effect of gas puffing LHW-plasma coupling, experiments of gas puffing from electron-side and ion-side on LHW-plasma are the plasma and LHW parameters are Ip = 400kA, Bt= 2T, and the launched spectrum of $N_{//}^{peak}$=2.1. It is performed with varying gas flow rate by investigating reflection coefficients and density measured by reciprocating probes. The electron density at the last closed flux surface (LCFS) and the RCs with different gas flow rate are plotted in Fig. 4 (a) and (b). It is shown that the density is higher and the RC is lower in the case of gas puffing from GIM_e, meaning that it is more efficient to improve density with GIM_e puffing. Further comparison (see Fig. 5) shows that for a same density at the LCFS, the RC in the case of GIM_e puffing is a little smaller than that in the case of GIM_i puffing, implying a higher density at the grill mouth when gas puffing from electron-side. This could be explained by the different movement direction of the electron after ionization. When puffing from GIM_e, the ionized electron moves toward to LHW antenna, whereas the one moves away from antenna when puffing from GIM_i. The electron moving to antenna will be useful to increase the grill density compared to the opposite direction, since the later is not magnetically connected to the grill due to some first components (e.g., limiter). Therefore, the density at the grill will be different even if with a same density at the LCFS, hence, leading to different RC.

4. High density experiments with LHCD

In order to improve CD efficiency at high density, experiments were performed by increasing density in one discharge with different operation conditions, i.e., poor and strong lithiation, density feedback with gas puffing and supersonic molecular beam injection (SMBI). For comparison, the launched LHW spectrum is $N_{//}^{peak}$ =2.1, the configuration is fixed double configuration, and local gas puffing from GIM_e is utilized in the experiments. The effect of driven current is estimated by the count of hard X-ray rate (60keV~200keV) normalized by the injected LHW power, which is proportional to current driven efficiency. The relationship between normalized bremsstrahlung emission and line averaged density (n_e) is shown in Fig. 6, indicating that with strong lithiation, the effect of current drive is much better than that poor one in the case of gas puffing. It is seen that in the strong lithized discharge, there is no sudden decrease of driven current, which deviates from the curve of $1/n_e$, until density up to $3.0\times10^{19}m^{-3}$, which is much larger the value of $2.0\times10^{19}m^{-3}$ in the poor lithiation. This is consistent with the previous studies [10] that lithium coating is beneficial to increase CD efficiency at high density, due to the low cycling and high temperature in the lithium condition. It is also seen that for a similar lithiation, the current drive effect with SMBI is worse than that with gas puffing. The reason for this is not clear. The possible reason for this is the SDF due to the larger density fluctuation with the SMBI experiments in the edge region (Fig. 7). In addition, in the SMBI case, a relative high neutral deuterium radiation is observed. This may result in high density in the edge (Fig.8), leading to the low CD effect possibly due to PDI or CA.

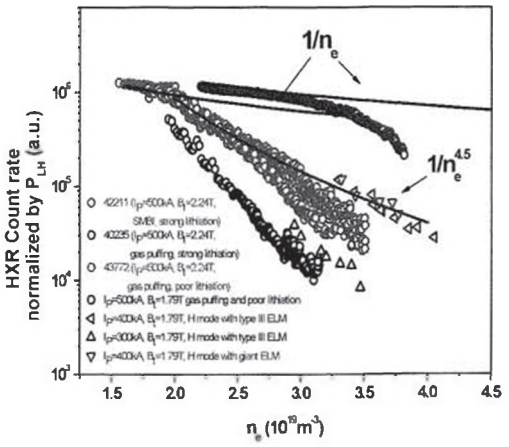

Fig.6 HXR vs density

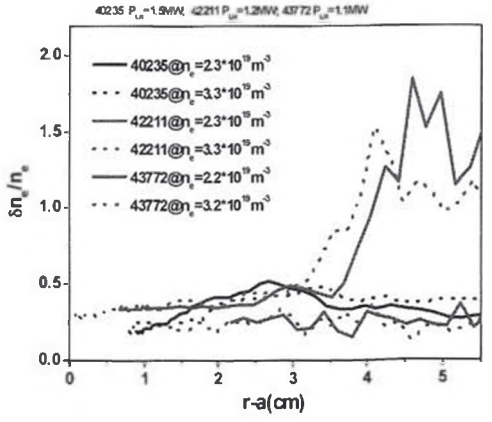

Fig.7Density fluctuation in SOL

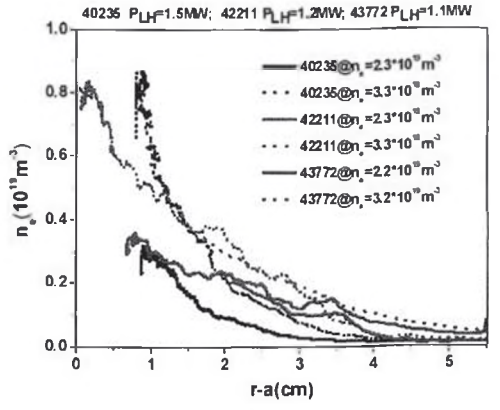

Fig.8 Density profile in SOL

Wave accessibility and PDI [22,23] have been suggested as possible explanations for the density limits observed on previous LHCD experiments. Since the same magnetic toroidal field and the LHW spectrum are fixed in the experiments, the discrepancy in sharp decay of bremsstrahlung emission is not due to wave accessibility. In addition, the dependences of CD effect on density are nearly consistent with the frequency of ion-cyclotron (IC) sideband (Fig. 9), measured by a RF loop antenna located outside the machine, implying the sharp decay of HXR counts is correlated with PDI [10].

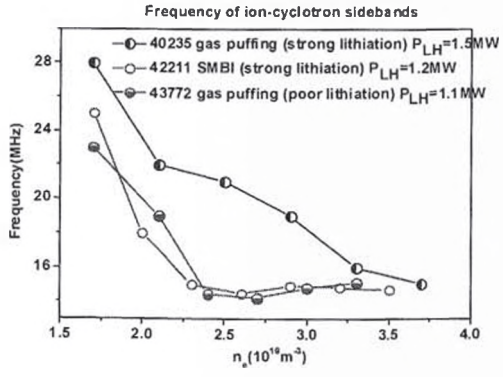

Fig.9 Frequency of IC sidebands

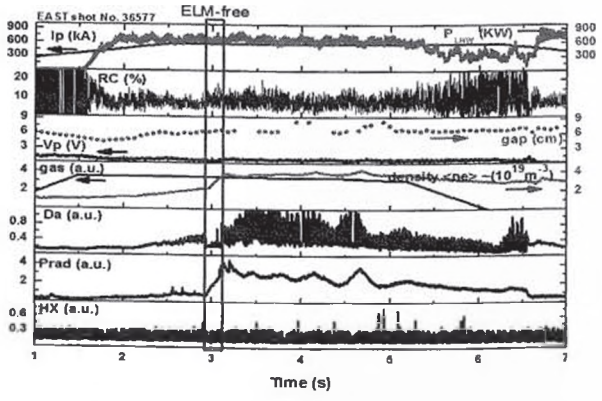

Fig.10 H-mode with gas puffing

Comparing the experimental data for different current and magnetic field, experiments also show that CD effect is better in higher plasma current or higher toroidal magnetic field, being in agreement with studies in Tore-Supra [24]. This is because high plasma current is favorable to increase temperature, hence improving CD efficiency. The effect of magnetic field on efficiency is mainly ascribed to wave accessibility condition. By further comparing the counts in L- and H-mode, it is seen that CD efficiency in H-mode is larger than that in L-mode for a same density. This means that efficiency at high density could be improved in H-mode plasma. As studied in FTU [7], this is mainly due to high temperature near edge region in H-mode associated with lithiation.

5. Investigation of H-mode experiments

Based on the above experiments, H-mode plasmas in EAST have been obtained by LHCD by means of using lithium coating and gas-puffing near LHW antenna in a wide range of parameters: Ip=0.4~0.8MA, B_t=1.35~1.81T, n_e=1.5~2.5x10^{19} m^{-3}, P_{LHW}>=0.5MW. An example of H-mode plasma sustained by LHCD alone is shown in Fig.10. Comparing L mode and ELM-free H-mode phases in Figs. 2 and 10, it is seen that there is no obvious change in RC(8%→10%) when L-H transition occurs in Fig. 10. The coupling deteriorates after switching off the gas puffing, thus leading to H-L transition. The strong variation of RC in H-mode can be explained by the ELMs, whereas the reason for variations in L-mode is not clear, possible due to density fluctuations. Unfortunately, no measurement is available in this discharge. Also, the radiation in Fig. 10 is much smaller than that in Fig. 2.

This indicates that lithiation and local gas puffing are effective to reduce radiation and improve LHW-plasma coupling, so as to obtain repeatable H-mode plasma.

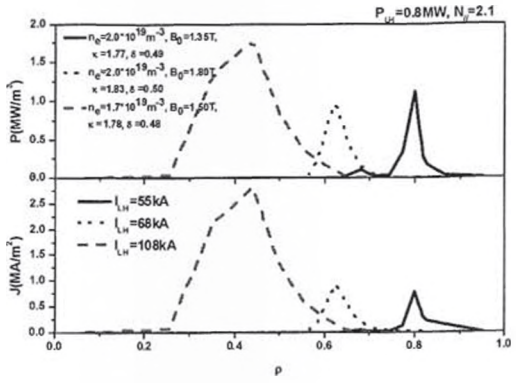

Fig.11 Simulation with C3PO/LUKE

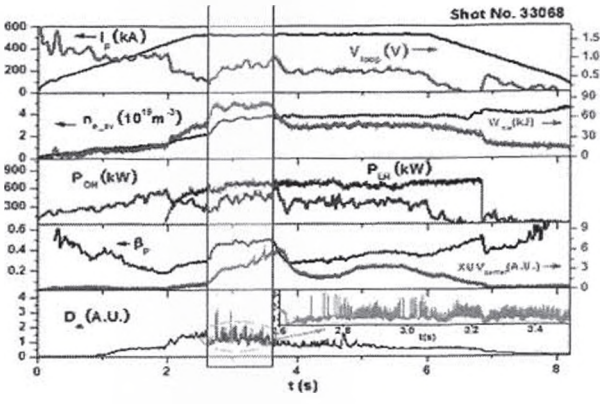

Fig.12 Typical H-mode waveform

Next, we would like to investigate dependence of H-mode on power deposition and driven current profile, which is calculated with a ray tracing and Fokker-Planck code of C3PO/LUKE [24]. Since magnetic field, plasma density and plasma configurations play important roles in determining LHW power deposition and current profile, three cases (1.n_e=2.0×$10^{19}$$m^{-3}$, B_t=1.35T, κ =1.77, δ =0.49; 2. n_e=2.0×$10^{19}$$m^{-3}$, B_0=1.8T, κ =1.83, δ =0.5; 3. n_e=1.7×$10^{19}$$m^{-3}$, B_t=1.5T, κ =1.78, δ =0.48) before L-H transition are selected from experiments for the calculation, where κ is the elongation and is δ the triangularity. Calculation results (Fig. 11) show the well known high dependency of the LH current drive calculations on plasma parameters(n_e, B_t, κ,δ) in the weak damping regime. The normalized peak power deposition ρ varies from 0.45 to 0.8, leading to different driven current profiles and total driven current, suggesting that L-H transition seems not so sensitive on current profile.

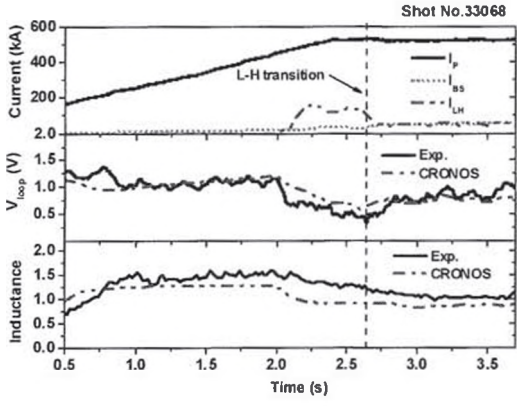

Fig.13 Simulations with CRONOS

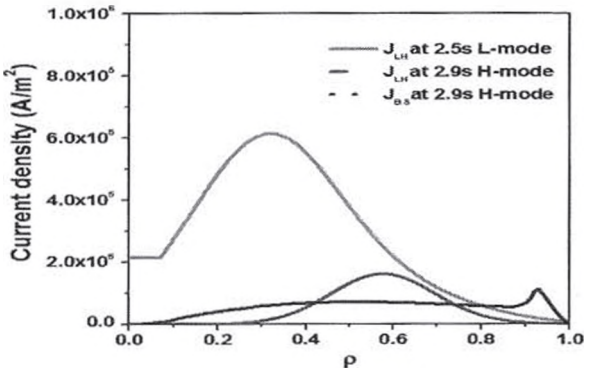

Fig.14 Simulation with CRONOS and LUKE

A typical H-mode discharge, characterized by the decrease of deuterium emission and ELM generation, and pedestal formation for the temperature and density profiles, is shown in Fig. 12. After L-H transition, plasma density increases quickly and stored energy is

up to 85kJ. The electron temperature decreases during the H phase, due to increasing density, leading to a little increase in loop voltage. Such change in loop voltage may be explained by the decrease of LH driven current due to decreasing Te and wave accessibility condition at high density during the H-mode phase. This can be also seen from I_{LH} (100kA in L and 50kA in H phase) (Fig. 13) and driven current profile (Fig. 14) predicted by the LUKE/C3PO and CRONOS [25,26], from which H-mode is reproduced with the initial equilibrium from EFIT and density from experiments. It is seen that Vp and inductance are qualitatively consistent between experiment and CRONOS (Fig.13). Though CRONOS results are preliminary, it offers an effective tool to investigate the experiment.

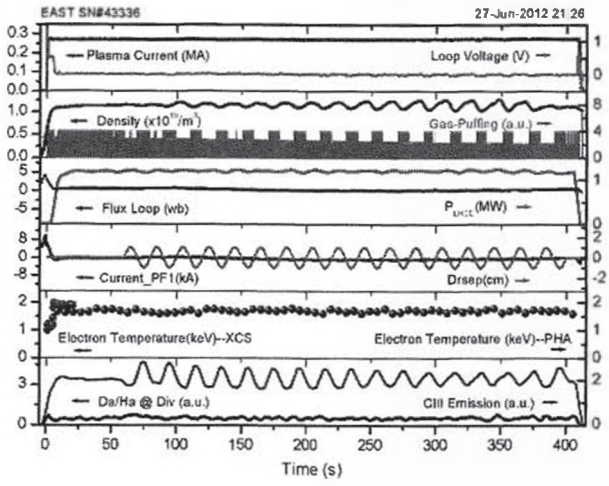

Fig.15 Long pulse over 400s in EAST

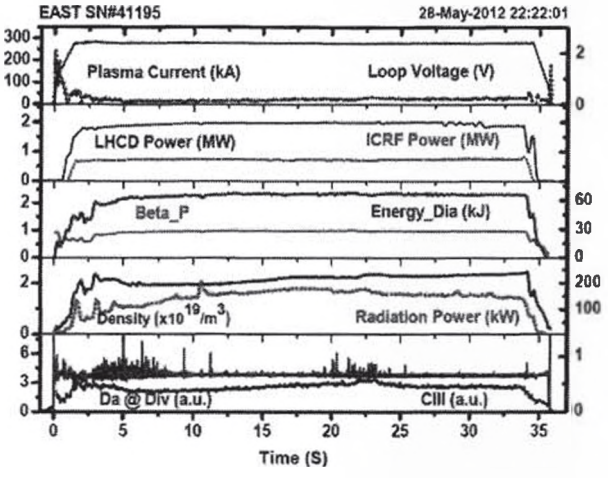

Fig.16 Long H-mode discharge (32s)

6. Demonstration of high performance, long pulse operation [27,28]

Long pulse plasma fully drive by LHW over 400s has been achieved in EAST (see Fig. 15) by carefully controlling heat exhaust and neutral recycling. Considering the present steady-state power handling capability ($2MW/m^2$), plasma configuration was varied from USN via DN to LSN during the discharge with sweeping strike point, thus minimizing divertor heat load, impurity influxex and plasma wall interaction. Plasma shape was real-time controlled so as to keep effective LHW coupling. LHW power is feedback controlled by flux. For a safe operation, all PF coil currents keep at a minimum level (<2kA), well below the critical current limit (14.5kA).

H-mode has now been extended with combination of LHCD and ICRH in EAST. Fig. 16 shows a typical long pulse H-mode (32s) discharge under the DN divertor configuration with the following parameters: Bt~1.9T, Ip=0.28MA, $ne\sim2.2\times10^{19}m^{-3}$, q_{95}~6.8, triangularity $\delta \sim 0.48$ and elongation $\kappa \sim 1.7$. It is dominated by small ELMS, with $H_{98,y2}$ ~0.8±0.1 and total injection of ~ 2.5MW. LHW and ICRF were applied during current ramp phase to reduce loop voltage and L-H transition occurred during the current flattop, accompanied with dithering phase. The plasma density and total radiation power in H-mode were

comparable to that in L-mode, suggesting possible high particle transport, especially no impurity accumulation in core plasma, which is beneficial for the sustainment of the long pulse H-mode.

7. Conclusion

Effect of local gas puffing from GIM_e and GIM_i of LHW antenna on LHW-plasma coupling is firstly investigated in EAST. Experimental results show that gas puffing from GIM_e is more favorable to improve coupling. Due to decreased coupled power together with the increasing radiation power in H-mode, H-L transition occurs. High density experiments with LHCD show that strong lithiation is useful for improve the density limit for LHCD. Studies indicate that the sharp decrease of current drive efficiency is correlated with PDI.

Using lithum coating and gas puffing from GIM_e of LHW antenna, H-mode plasma is obtained by LHCD in a wide range of parameters: Ip=0.4~0.8MA, B_t=1.35~1.81T, n_e=1.5~2.5x10^{19} m^{-3}, P_{LHW}>=0.5MW. Simulation shows that central and large driven current seems not a necessary condition for H-mode plasma. H-mode is reproduced by CRONOS, suggesting it can offer a tool to explain experiments. Long pulse plasmas (>400s L mode and >30s H-mode) have been achieved.

Acknowledgements: This work is supported by the National Magnetic Confinement Fusion Science Program of China (Grant No 2010GB105000), the National Natural Science Foundation of China under Grant No. 11175206, 10875149 and 10928509.

References:

[1] Fisch N.J. 1978 *Phys. Rev. Lett.* **41** 873.

[2] Bernabei S. *et al* 1982 *Phys. Rev. Lett.* **49** 1255.

[3] Fisch N.J. 1987 *Rev. Mod. Phys.* **59** 175.

[4]N. J. Fisch and A. H. Boozer 1980 *Phys. Rev. Lett.* **45** 720.

[5]Pericoli-Ridolfini V., et al 1994 *Nucl. Fusion* **34** 469.

[6]Cesario R., *et al* 2011 *Plasma Phys. Control. Fusion* **53** 085011.

[7]Cedario R., et al 2010 *Nature Commun.* http://dx.doi.org/10.1038/ncomms1052

[8]Wallace, G.M., *et al* 2010 *Phys. Plasmas* **17** 082508.

[9]Bonoli P.T., and Englade, R.C. 1986 *Phys. Fluids* **29** 2937.

[10] Liu C.S., and TRIPATHI, V.K. 1986 Phys. Rep. 130 143.

[11] Peysson Y., Decker J., Morini L., et al 2011 *Plasma Phys. Contr. Fusion* **53** 124028.

[12] Wagner F. *et al* 1982 *Phys. Rev. Lett.* **49** 1408.

[13]Steinmetz K. *et al* 1987 *Phys. Rev. Lett.* **58** 124.

[14] Lohr J.M., *et al* 1988 *Phys. Rev. Lett.* **60** 2630.

[15] Tsuji S., *et al* 1990 *Phys. Rev. Lett.* **64** 1023.

[16] Wan Y.X. *et al* 2000 *Nucl. Fusion* **40** 1057.

[17] Weng P.D. *et al* 2005 *Fusion Eng. Des.* **75–79** 143.

[18] Fu P. *et al* 2006 *Nucl. Fusion* **46** S85.

[19] Liu X.N. *et al* 2006 *Nucl. Fusion* **46** S90.

[20] Wan Y.X. *et al* 2006 *Plasma Sci. Technol.* **8** 253.

[21] Brambilla M. 1976 *Nucl. Fusion* **16** 47.

[22]Takase Y., Porkolab M., Schuss J. J., *et al* 1985 *Phys. Fluids* **28** 983.

[23] Hooke W. 1984 *Plasma Phys. Contr. Fusion* **26** 133.

[24] Peysson Y. and the Tore Supra Team 2001 *Nucl. Fusion* **41** 1703.

[25]Peysson Y. and Decker J. 2008 *AIP Conf. Proc.* **1069** 176.

[26] Artaud J. F., *et al* 2010, *Nucl. Fusion* **50** 043001.

[27] Wan B N et al, 2012 Fusion energy conference OV/2-5.

[28] Guo H Y et al, 2012 Fusion energy conference EX/P5-15.